

Dielectric response of disordered $\text{Pb}(\text{Sc}_{1/2}\text{Ta}_{1/2})\text{O}_3$ single crystal under hydrostatic pressure

A. Hilczer and M. Szafranski*

Faculty of Physics, Adam Mickiewicz University, Poznań, Poland

(Received 18 May 2008; final version received 29 May 2008)

The effect of hydrostatic pressure on the dielectric response of $\text{Pb}(\text{Sc}_{1/2}\text{Ta}_{1/2})\text{O}_3$ single crystal with the degree of order $S=0.16$ has been studied. At elevated pressures the dielectric anomaly characteristic of ferroelectric relaxors is shifted to lower temperatures, its amplitude decreases and the relaxor peak becomes more diffused. In the pressure range studied up to 0.75 GPa, the temperature dependencies of the characteristic relaxation time obey the Vogel–Fulcher law. It has been found that the Vogel–Fulcher temperature decreases with increasing pressure while the activation energy of the dipolar entities increases. This increase can be ascribed to the pressure-induced changes in the atom–atom and dipolar interactions, resulting in the increased energy barriers for dipolar fluctuations.

Keywords: ferroelectric relaxors; lead scandium tantalite; dielectric response; hydrostatic pressure

1. Introduction

Complex perovskites $A(B'_{1-x}B''_x)\text{O}_3$ with B' and B'' of different ionic radii and valencies exhibit relaxor properties mirrored in a broad and frequency-dependent dielectric anomaly and a local polarisation that persists a few hundred Kelvins above the temperature of the permittivity maximum $T_{\varepsilon'_{\max}}$ [1–3]. The origin of these properties is complex and related to the presence of both random fields and polar nanoregions (PNRs). In the $A(B'_{1-x}B''_x)\text{O}_3$ type relaxors the random fields originate from the lattice defects as well as from the local elastic and electric fields, created as a result of the difference in the ionic radii and electric charges between the B' and B'' ions [4,5]. The B -type ion substitution in $\text{Pb}(B'_{1/2}B''_{1/2})\text{O}_3$ perovskites modifies the lattice energy, which can lead to a local ordering in the form of chemical domains, where the B^{3+} and B^{5+} ions are located on the alternating lattice planes. In $\text{Pb}(\text{Sc}_{1/2}\text{Ta}_{1/2})\text{O}_3$ and $\text{Pb}(\text{Sc}_{1/2}\text{Nb}_{1/2})\text{O}_3$, (abbreviated as PST and PSN, respectively) the Sc^{3+} ions and Ta^{5+} or Nb^{5+} ions can be either randomly distributed at the B -sites of the perovskite lattice or segregated in the $\{111\}$ planes [6–8]. The average structure of PST, with Sc^{3+} and Ta^{5+} ions randomly disordered, is cubic with $Pm\bar{3}m$ space group, whereas the ordering of the Sc^{3+} ions and Ta^{5+} ions in the alternating $\{111\}$ planes results in a doubling of the basic perovskite unit cell and $Fm\bar{3}m$ space group [9–11]. The chemical order of Sc^{3+} and Ta^{5+} is reflected in the X-ray diffraction pattern by the occurrence of the superstructure reflections of the $\{h+1/2, k+1/2, l+1/2\}$ type. The absence of the

*Corresponding author. Email: masza@amu.edu.pl

superstructure reflections points to a random distribution of the ions [9,12]. It has been shown that at room temperature PST can exist in different states of order, associated with different properties. As the degree of order can be controlled by thermal treatment [9,12–14], the properties of this compound can be easily tuned. The PST single crystals, in which the volume of the chemical order amounted to 35% and 29%, have been found to exhibit classical relaxor properties [13,15,16], while at higher order of 80% a spontaneous relaxor-to-ferroelectric phase transition has been observed [13,15]. Although the average symmetry of the relaxor state is cubic, the local symmetry is broken due to the formation of polar nano-regions, which persist up to the Burns temperature $T_B = 600$ K [1–3,15]. It should be stressed that the behaviour of PST ceramics is different than that of the single crystals [4,12–14,17]. In contrast to the disordered PST crystals, the ceramic samples were reported to show relaxor properties at room temperature and a spontaneous first-order relaxor-to-ferroelectric phase transition at ~ 270 K. Moreover, it was observed that lead vacancies inhibited the transition [17]. On the other hand, the ceramics ordered at 90% underwent a paraelectric-to-ferroelectric phase transition at ~ 298 K [17,5]. As both the valencies and the ionic radii of Ta^{5+} and Nb^{5+} ions are practically the same [18], one can expect a similar stability of the ordered and disordered states of PST and PSN compounds [14,17,5,19]. It appears that both PST and PSN are close to the stability limit between the randomly distributed Sc^{3+} and $\text{Ta}^{5+}/\text{Nb}^{5+}$ ions, and the ordered state. Thus, in these materials the equilibrium between the long- and the short-range interactions can be easily varied by changing the degree of order. The interactions can also be modified by external thermodynamic factors like electric field or pressure. Samara has shown that application of pressure is especially useful for studying the nature and dynamics of PNRs, as it does not disturb the chemical composition of the substance and the distribution of the lattice defects [2,20,21].

The studies of dielectric response of PST under high pressure have been rather fragmentary. The measurements were performed only at 1 and 100 kHz for the single-crystal and ceramic samples, respectively [22]. The authors reported a downward shift of the dielectric anomaly with $\Delta T/\Delta p = -36$ K GPa $^{-1}$ for disordered crystal ($S = 0.35$) and $\Delta T/\Delta p = -38$ K GPa $^{-1}$ for disordered ceramics ($S = 0.40$). The ordered samples exhibited slightly smaller pressure effect characterized by the coefficients $\Delta T/\Delta p = -20$ K GPa $^{-1}$ for the crystal ($S = 0.80$) and $\Delta T/\Delta p = -31$ K GPa $^{-1}$ for the ceramics ($S = 0.85$). The lack of detailed high-pressure investigation of the dielectric response of PST has motivated us to undertake this study.

2. Experimental

2.1. Sample preparation and characterisation

A sample oriented perpendicularly to the crystallographic [111] direction was cut from the as-grown PST single crystal with cubic morphology. The sample (0.65 mm thick and 1.5 mm 2 in area) was polished with diamond pastes, and its large surfaces were covered with gold sputtered electrodes.

The degree of order of the PST crystal was determined by X-ray diffraction method [9] using the following formulae:

$$S_1^2 = \frac{[I_{1/21/21/2}/I_{100}]_{\text{exp}}}{[I_{1/21/21/2}/I_{100}]_{S=1}} \quad \text{and} \quad S_2^2 = \frac{[I_{3/21/21/2}/I_{111}]_{\text{exp}}}{[I_{3/21/21/2}/I_{111}]_{S=1}}, \quad (1)$$

where $I_{1/21/21/2}$ and $I_{3/21/21/2}$ denote the integrated intensities of the (1/2 1/2 1/2) and (3/2 1/2 1/2) superstructure reflections, I_{100} and I_{111} are the integrated intensities of the fundamental (100) and (111) reflections, and $[I_{1/21/21/2}/I_{100}]_{S=1} = 1.33$ and $[I_{3/21/21/2}/I_{111}]_{S=1} = 0.59$ are the intensity ratios calculated for the $Fm\bar{3}m$ fully-ordered structure.

The reflections were collected at room temperature using a KUMA CCD four-circle X-ray diffractometer operating with graphite-monochromated Mo-K α radiation. The integrated intensities $I_{1/21/21/2}$, $I_{3/21/21/2}$, I_{100} and I_{111} were determined as the average values of 10 superstructure reflections of the (1/2 1/2 1/2) type, 52 superstructure reflections of the (3/2 1/2 1/2) type, 8 fundamental reflections of the (100) type and 17 fundamental reflections of the (111) type, respectively. Using Equation (1), $S_1 = 0.168$ and $S_2 = 0.143$ have been determined. The average value of S_1 and S_2 was assumed as the degree of order of the sample $S = 0.16$.

2.2. Measurements

Dielectric response of the PST crystal was measured in the temperature range 80–350 K, on heating and cooling. The measurements were performed at ambient pressure and under hydrostatic pressures up to 0.75 GPa, in the frequency range 1 kHz–1 MHz, with a computer controlled HP 4192A Impedance Analyzer. The measuring electric field strength was of 7.5 V cm⁻¹. After the pressure was applied at room temperature, the sample was heated at a rate of 1 K min⁻¹ to 350 K. Thereafter the dielectric measurements were performed on cooling to 150 K and then on heating to 350 K at the rate 1 K min⁻¹. For pressure measurements the sample was placed in a beryllium–copper pressure cell, the temperature of which was controlled. The pressure was generated by a GCA-10 gas compressor (Unipress, Poland) and helium was used as the pressure transmitting medium. The pressure was measured by means of a calibrated manganin gauge with an accuracy of ± 0.01 GPa and the temperature of the sample was measured with an accuracy of ± 0.05 K using a copper-constantan thermocouple placed in a close vicinity of the sample.

3. Results and discussion

3.1. Dielectric response of the PST crystal at ambient pressure

The temperature dependencies of the real and imaginary parts of the complex electric permittivity of PST measured at ambient pressure are shown in Figure 1. These measurements were performed on cooling. At atmospheric pressure the maxima occur at: $T_{\epsilon'_{\max}}(1\text{kHz}) = 261.3$ K, $T_{\epsilon'_{\max}}(1\text{MHz}) = 274.8$ K, $T_{\epsilon''_{\max}}(1\text{kHz}) = 238.3$ K and $T_{\epsilon''_{\max}}(1\text{MHz}) = 255.2$ K. The dielectric response of the crystal shows a single frequency-dependent anomaly both in $\epsilon'(f, T)$ and $\epsilon''(f, T)$, without any sign of a spontaneous transformation to the ferroelectric phase. Below this anomaly, in the low-temperature range, a continuous decrease in the permittivity and a dielectric dispersion are apparent (Figure 2).

Figure 3 illustrates the temperature hysteresis between the cooling and the subsequent heating runs. The difference in the permittivity values occurs in the vicinity of $T_{\epsilon'_{\max}}$ and persists at low temperatures. The effect is especially distinct for lower frequencies. A similar but smaller thermal hysteresis was observed earlier at 1 kHz for the PST crystal with $S = 0.29$ [16]. The effect can originate from some kind of long-range ordering at low temperatures and spontaneous aging of the sample. The aging processes play an important role in ferroelectric relaxors and usually are mirrored in the low-frequency dielectric response [23,24].

3.2. Dielectric response of the PST crystal under hydrostatic pressure

The aging process in ferroelectric relaxors is strongly dependent on the thermal history of the sample [23,24]. The application of hydrostatic pressure increases the internal energy of the system and therefore one can also expect an aging effect after releasing the pressure. Figure 4 shows the temperature dependencies of the permittivity measured

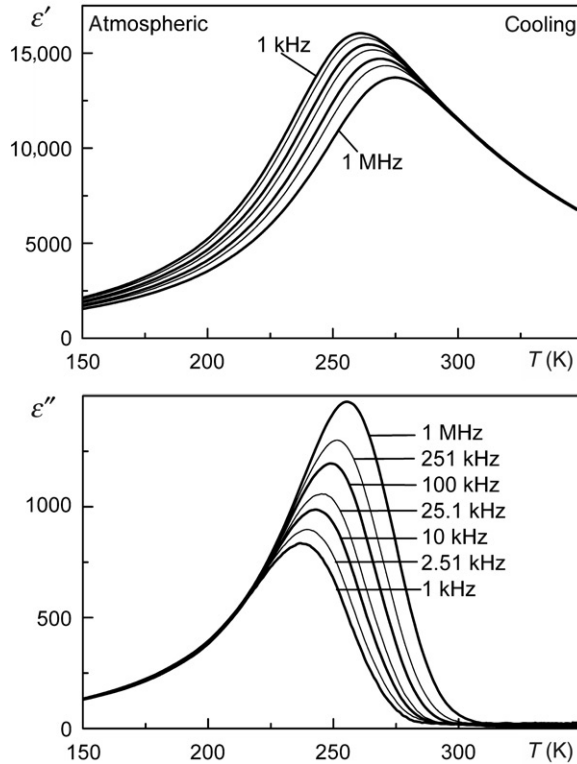


Figure 1. Dielectric response of the PST single crystal measured at different frequencies along the [111] direction on cooling the sample.

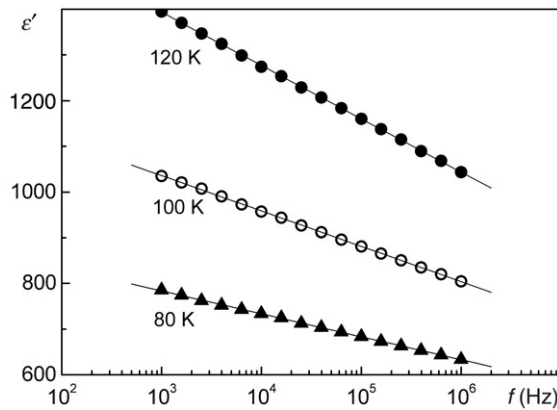


Figure 2. The low-temperature frequency dispersion of the real part of electric permittivity in the PST crystal.

at 1 kHz and 1 MHz for 'virgin' sample and for sample subjected to the pressure of 0.75 GPa. Then the pressure was released and a series of measurements was performed with different time interval separating the subsequent runs. The most pronounced decrease in the permittivity value is seen in the vicinity of $T_{\epsilon'_{\max}}$. The inset in Figure 4 shows that the aging rate is higher for the low-frequency response. The aging effect related to the application of hydrostatic pressure is more profound than that observed after thermal annealing of the sample. At the frequency of 1 kHz the change in the maximum permittivity after 264h of the pressure releasing amounted to 12%, whereas after the same period of time the permittivity of thermally annealed sample decreased by 4%.

In order to minimize the contribution of spontaneous aging of the sample to the pressure effect, further in this article we compare and present only the results of measurements obtained on cooling from 350 to 150 K. The effect of hydrostatic pressure on the dielectric response of disordered PST single crystal is shown in Figure 5.

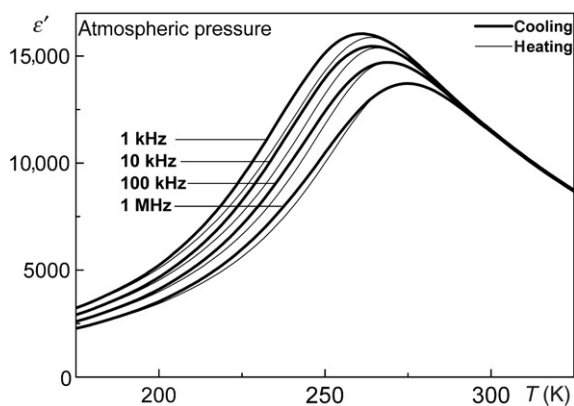


Figure 3. Temperature hysteresis between the cooling and the heating runs of $\epsilon'(T)$ for various frequencies.

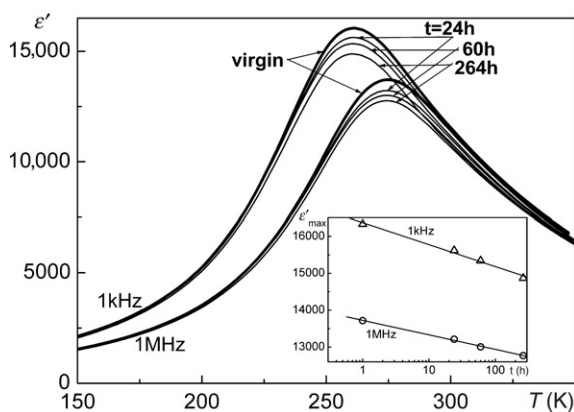


Figure 4. Time-dependent changes in the dielectric response of PST after releasing the pressure. The inset shows the maximum value of the permittivity measured at 1 kHz and 1 MHz as a function of time.

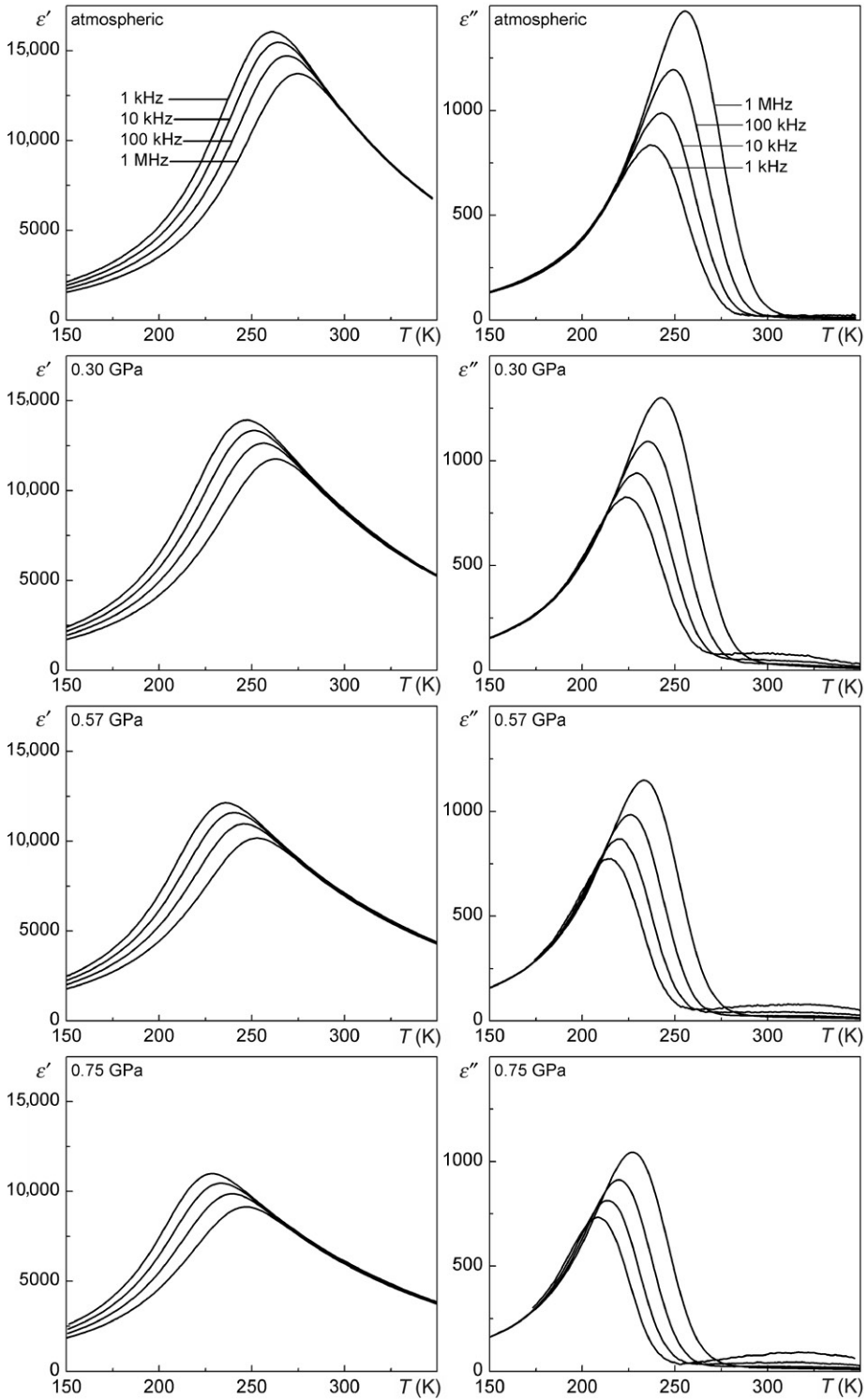


Figure 5. The real and imaginary parts of the complex electric permittivity of PST measured as a function of temperature and frequency at different pressures.

The dielectric anomaly shifts to lower temperatures with increasing pressure, similar to those reported earlier for other perovskite ferroelectric relaxors [2,20–22,25–32]. The temperatures of the permittivity maxima, plotted in Figure 6, decrease linearly and can be described by the following relations:

$$\begin{aligned}dT_{\epsilon'_{\max}}(1\text{ kHz})/dp &= (-43.0 \pm 0.7)\text{K GPa}^{-1} \\dT_{\epsilon'_{\max}}(1\text{ MHz})/dp &= (-37.9 \pm 0.7)\text{K GPa}^{-1}.\end{aligned}\quad (2)$$

Hydrostatic pressure affects not only the temperature of the dielectric anomaly, but also its magnitude and shape. In Figure 7 we plotted the normalised values of permittivity

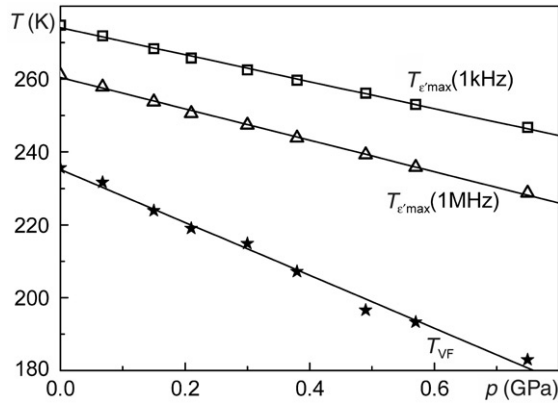


Figure 6. The influence of pressure on $T_{\epsilon'_{\max}}$ and T_{VF} .

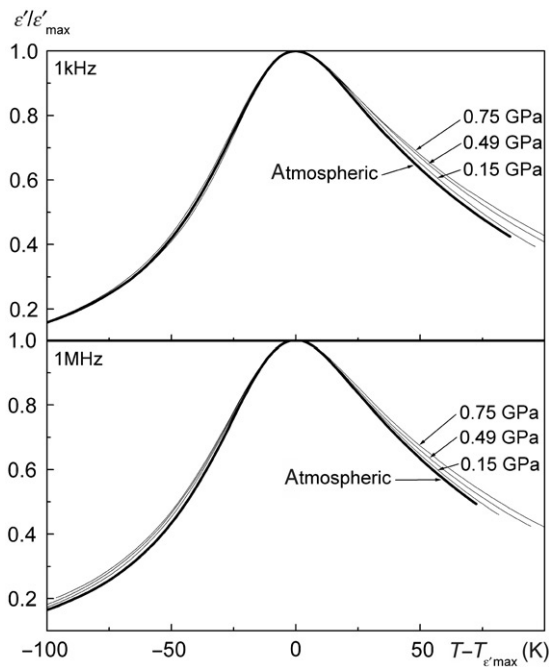


Figure 7. Normalized permittivity $\epsilon'/\epsilon'_{\max}$ at 1 kHz and 1 MHz plotted for selected pressures as a function of reduced temperature $T - T_{\epsilon'_{\max}}$.

$\epsilon'/\epsilon'_{\max}$ as a function of $T - T_{\epsilon'_{\max}}$. The curves obtained for different pressures do not form a single master curve, as observed earlier for $\text{Pb}(\text{Mg}_{1/3}\text{Nb}_{2/3})_{0.7}\text{Ti}_{0.3}\text{O}_3$ [33]. As seen in Figure 7, the pressure mainly influences the dielectric permittivity above $T_{\epsilon'_{\max}}$. To characterize the pressure-induced changes in this high-temperature side we used a Lorentz-type equation [34]:

$$\frac{\epsilon'_A}{\epsilon'} = 1 + \frac{(T - T_A)^2}{2(\delta_A)^2}, \tag{3}$$

where $T_A < T_{\epsilon'_{\max}}$, $\epsilon'_A > \epsilon'_{\max}$ and δ_A are the parameters fitted to experimental data. The parameter δ_A can be used as a measure of the anomaly diffuseness. Examples of the fittings for the data measured at various pressures are shown in Figure 8. The diffuseness parameter δ_A derived from the fits is plotted as a function of pressure in Figure 9. The linear increase of δ_A with increasing pressure [$d\delta_A/dp = (14.7 \pm 0.4)\text{K GPa}^{-1}$] indicates that, in the studied pressure range, the hydrostatic pressure grounds the relaxor state.

To obtain more information on the dynamics of the PNRs at elevated pressures, we determined the characteristic relaxation times ($\tau = 1/2\pi f$, where f is the frequency of the

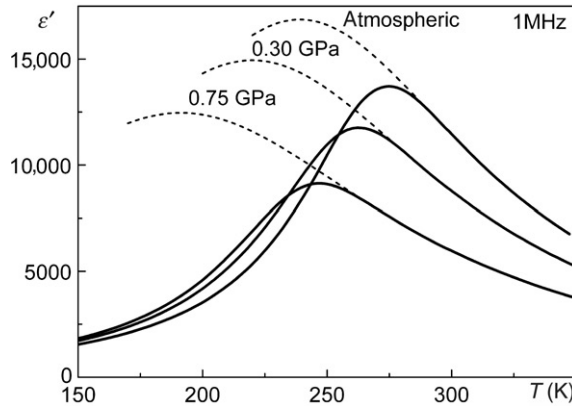


Figure 8. The 1 MHz temperature dependencies of the electric permittivity at different pressures (solid lines) and the fits (dotted lines) to Equation (3).

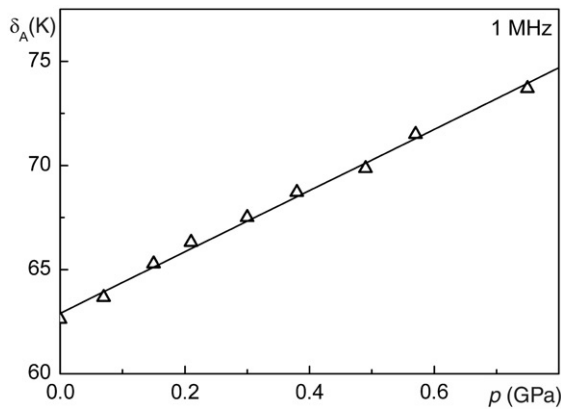


Figure 9. Pressure dependence of the diffuseness parameter δ_A calculated from Equation (3).

electric measuring field) in relation to the corresponding $T_{e'_{\max}}$. The temperature dependencies of the relaxation times (Figure 10a) were described using the Vogel–Fulcher equation [2,3]:

$$\tau(T) = \tau_{\text{VF}} \exp\left(\frac{-B}{T - T_{\text{VF}}}\right), \quad (4)$$

where τ_{VF} is the inverse attempt frequency, T_{VF} the temperature at which the relaxation time diverges and B the activation energy. The frequency range of the experimental data available was limited to 3 decades, and therefore the parameters obtained from the fits may be weighed with large uncertainties. Nevertheless, both T_{VF} and B show systematic changes with increasing pressure. At elevated pressures the temperature T_{VF} shifts linearly towards lower temperatures (Figure 6), while the activation energy B increases continuously from ~ 500 K at atmospheric pressure to ~ 1100 K at 0.75 GPa, as illustrated in Figure 10(b).

The pressure effect is also responsible for a considerable decrease in the permittivity values. Figure 11 shows the pressure dependence of the electric permittivity measured at

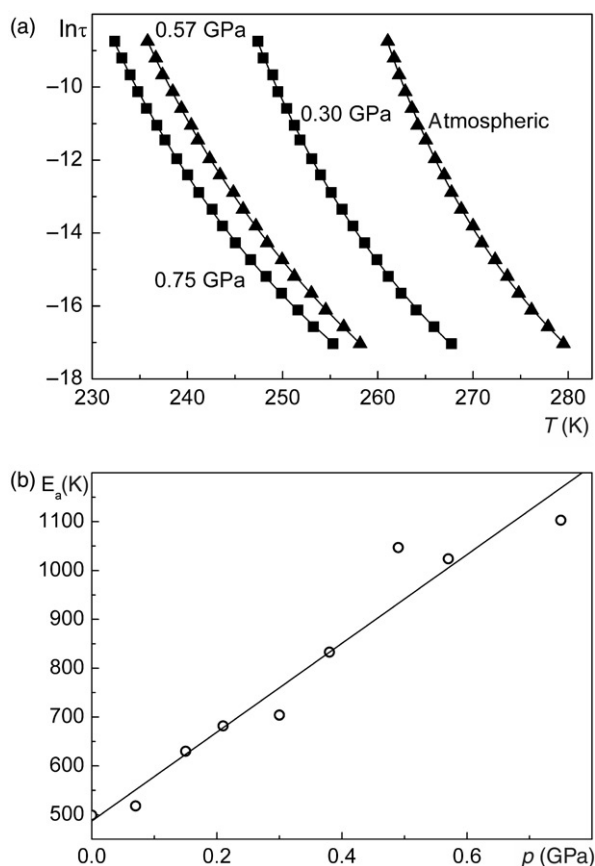


Figure 10. Temperature dependencies of the relaxation time at various pressures (a), the solid lines represents the best fits to the Vogel–Fulcher law, Equation (4), and pressure dependence of the activation energy (b).

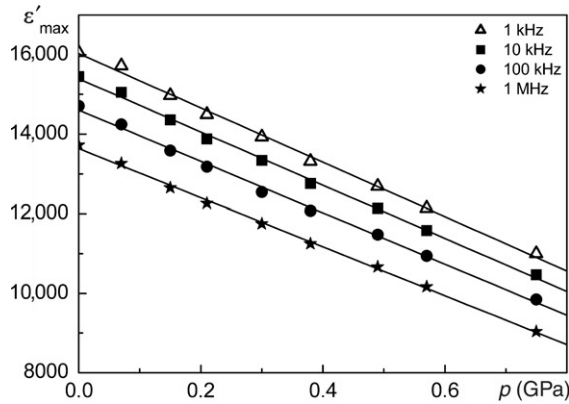


Figure 11. Pressure dependence of the maximum permittivity values at 1, 10, 100 kHz and 1 MHz.

$T_{\epsilon'_{\max}}$ for various frequencies on cooling. Although the pressure coefficients of these dependencies are slightly different for particular frequencies, the pressure-induced relative changes are very similar. For example, for 1 kHz and 1 MHz they amount to $(-42.6 \pm 0.8)\% \text{ GPa}^{-1}$ and $(-44.2 \pm 0.8)\% \text{ GPa}^{-1}$, respectively.

4. Conclusions

The results of this study indicate that hydrostatic pressure considerably affects the dielectric response of the PST single crystal with the degree of order $S=0.16$. In general, this influence is very similar to that reported earlier for other mixed perovskites. The dielectric anomaly is shifted to lower temperatures and its magnitude decreases with increasing pressure. The diffuseness parameter δ_A , derived from the fitting of the experimental data to the Lorenz-type equation, exhibits a much stronger pressure dependence than that observed for $PMN-0.30PT$ single crystal [33] or PSN ceramics [32]. Moreover, at elevated pressures the Vogel-Fulcher temperature T_{VF} decreases more quickly than $T_{\epsilon'_{\max}}$. Thus, under pressure the non-ergodic relaxor state is grounded and enhanced in T -range. It is worth noting that the activation energy B , calculated from the fittings of the Vogel-Fulcher equation to the experimental data, increases with increasing pressure. A similar behaviour of the activation energy was observed in our previous high-pressure study of PSN ceramics [32]. On the other hand, Samara et al. have suggested a reverse pressure dependence of this parameter for PSN single crystal [26], for La-substituted lead zirconate/titanate [27] and for Ba- and Bi-substituted lead zirconate/titanate [35]. The authors argued that the decrease in the activation energy occurs as a result of a reduced size of the PNRs. However, it should be stressed that pressure modifies not only the size of the dipolar entities but also dipolar and interatomic interactions. The latter effect can cause an increase in the energy barriers hindering the dipolar motions. To support this idea further high-pressure studies including a wider frequency range are desired.

Acknowledgements

The authors are grateful to Prof. R. Blinc for providing the PST crystal and Prof. A. Pietraszko for his help in determining the degree of the crystal order. This work was supported by the Polish Committee of Scientific Research, Grant No. 1 P03B 110 27.

References

- [1] L.E. Cross, *Relaxor Ferroelectrics*, *Ferroelectrics* 76 (1987), pp. 241–267.
- [2] G.A. Samara, *Ferroelectricity revisited—advances in materials and physics*, in *Solid State Physics* 56, H. Ehrenreich and F. Spaepen, eds., Academic Press, New York, 2001, pp. 239–459.
- [3] A.A. Bokov and Z.-G. Ye, *Recent progress in relaxor with perovskite structure*, *J. Mater. Sci.* 41 (2006), pp. 31–52.
- [4] F. Chu, I.M. Reaney, and N. Setter, *Investigation of relaxor that transform spontaneously into ferroelectrics*, *Ferroelectrics* 151 (1994), pp. 343–348.
- [5] F. Chu, I.M. Reaney, and N. Setter, *Spontaneous (zero-field) relaxor-to-ferroelectric-phase transition in disordered $Pb(Sc_{1/2}Nb_{1/2})O_3$* , *J. Appl. Phys.* 77 (1995), pp. 1671–1676.
- [6] C.A. Randall, D.J. Barber, and R.W. Whatmore, *In-situ TEM experiments on perovskite-structured ferroelectric relaxor materials*, *J. Microscopy* 145 (1987), pp. 275–291.
- [7] C. Randall, D. Barber, R. Whatmore, and P. Groves, *Short-range order phenomena in lead-based perovskites*, *Ferroelectrics* 76 (1987), pp. 277–282.
- [8] L.A. Bursill, *Atomic resolution imaging of ferroelectric domains*, *Ferroelectrics* 191 (1997), pp. 129–134.
- [9] C.G.F. Stenger and J.A. Burggraaf, *Order-disorder reactions in the ferroelectric perovskites $Pb(Sc_{1/2}Nb_{1/2})O_3$ and $Pb(Sc_{1/2}Ta_{1/2})O_3$. I. Kinetics of the Ordering Process*, *Phys. Stat. Sol.* (a) 61 (1980), pp. 275–285.
- [10] K.Z. Baba-Kishi and D.J. Barber, *Transmission electron microscope studies of phase transitions in single crystals and ceramics of ferroelectric $Pb(Sc_{1/2}Ta_{1/2})O_3$* , *J. Appl. Cryst.* 23 (1990), pp. 43–54.
- [11] P.M. Woodward and K.Z. Baba-Kishi, *Crystal structures of the relaxor oxide $Pb_2(ScTa)O_6$ in the paraelectric and ferroelectric states*, *J. Appl. Cryst.* 35 (2002), pp. 233–242.
- [12] F. Chu, M. Daglish, and N. Setter, *The reversibility of ordering effects in $Pb(Sc_{1/2}Ta_{1/2})O_3$ ceramics*, in *Third Euro-Ceramics vol. 2: Properties of Ceramics*, P. Duran and J.F. Fernandez, eds., Faenza Editrice Iberica S.L., Castellon de la Plana, 1993, pp. 91–96.
- [13] N. Setter and L.E. Cross, *The role of B-site cation disorder in diffuse phase transition behaviour of the perovskite ferroelectrics*, *J. Appl. Phys.* 51 (1980), pp. 4356–4360.
- [14] F. Chu, N. Setter, and A.K. Tagantsev, *The spontaneous relaxor-ferroelectric transition of $Pb(Sc_{1/2}Ta_{1/2})O_3$* , *J. Appl. Phys.* 74 (1993), pp. 5129–5134.
- [15] D. Viehland and J.-F. Li, *Dependence of the glasslike characteristics of relaxor ferroelectrics on chemical ordering*, *J. Appl. Phys.* 75 (1994), pp. 1705–1709.
- [16] J.-H. Ko, F. Jiang, S. Kojima, T.A. Shaplygina, and S.G. Lushnikov, *Linear and nonlinear dielectric susceptibilities of disordered lead scandium tantalate*, *J. Phys. Condens. Matter* 13 (2001), pp. 5449–5462.
- [17] F. Chu, G.R. Fox, and N. Setter, *Dielectric properties of complex perovskite lead scandium tantalate under dc Bias*, *J. Am. Ceram. Soc.* 81 (1998), pp. 1577–1582.
- [18] R.D. Shannon, *Revised effective ionic radii and systematic studies of interatomic distances in halides and chalcogenides*, *Acta Cryst. A* 32 (1976), pp. 751–767.
- [19] (a) C. Malibert, B. Dkhil, J.M. Kiat, D. Durand, J.F. Bézar, and A. Spasojevic-de Biré, *Order and disorder in the relaxor ferroelectric perovskite $PbSc_{1/2}Nb_{1/2}O_3$ (PSN): Comparison with simple perovskites $BaTiO_3$ and $PbTiO_3$* , *J. Phys. Condens. Matter* 9 (1997), pp. 7485–7500; (b) R. Haumont, J. Carreaud, P. Gemeiner, B. Dkhil, C. Malibert, A. Al-Barakat, L. Bellaiche, and J.M. Kiat, *Polar and chemical order in relation with morphotropic phase boundaries and relaxor behaviour in bulk and nanostructured PSN–PT*, *Phase Transit.* 79 (2006), pp. 123–134.
- [20] G.A. Samara, *The relaxational properties of compositionally disordered ABO_3 perovskites*, *J. Phys. Condens. Matter* 15 (2003), pp. 367–411.
- [21] G.A. Samara, *Pressure induced crossover and mechanism for the ferroelectric-to-relaxor (glass-like) transition in compositionally-disordered soft mode systems*, *Ferroelectrics* 274 (2002), pp. 183–202.

- [22] N. Setter and L.E. Cross, *Pressure dependence of the dielectric properties of $Pb(Sc_{1/2}Ta_{1/2})O_3$* , Phys. Stat. Sol. (a) 61 (1980), p. 75.
- [23] W.A. Schulze and K. Ogino, *Review of literature on aging of dielectrics*, Ferroelectrics 87 (1988), pp. 361–377.
- [24] E.V. Colla, L.K. Chao, and M.B. Weissman, *Multiple aging mechanisms in relaxor ferroelectrics*, Phys. Rev. B 63 (2001), pp. 134107–1–10.
- [25] G.A. Samara and E.L. Venturini, *Ferroelectric/relaxor crossover in compositionally disordered perovskites*, Phase Transit. 79 (2006), pp. 21–40.
- [26] E. Venturini, R.K. Grubbs, G.A. Samara, Y. Bing, and Z.-G. Ye, *Ferroelectric and relaxor properties of $Pb(Sc_{1/2}Nb_{1/2})O_3$: Influence of pressure and biasing electric field*, Phys. Rev. B 74 (2006), pp. 064108–1–9.
- [27] G.A. Samara, *Pressure-induced crossover from long- to short-range order in compositionally disordered soft mode ferroelectrics*, Phys. Rev. Lett. 77 (1996), pp. 314–317.
- [28] G.A. Samara, *Pressure as a probe of the glassy properties of compositionally disordered soft mode ferroelectrics: $(Pb_{0.82}La_{0.12})(Zr_{0.40}Ti_{0.60})O_3$ (PLZT 12/40/60)*, J. Appl. Phys. 84 (1998), pp. 2538–2547.
- [29] G.A. Samara, E.L. Venturini, and V.H. Schmidt, *Dielectric properties and phase transitions of $[Pb(Zn_{1/3}Nb_{2/3})O_3]_{0.905}(PbTiO_3)_{0.095}$: Influence of pressure*, Phys. Rev. B 63 (2001), pp. 184104–1–11.
- [30] W. Nawrocik, P. Czarnecki, A. Hilczer, and R. Blinc, *Effect of hydrostatic pressure on the dielectric response of $Pb(Mg_{1/3}Nb_{2/3})O_3$ relaxor*, Phase Transit. 76 (2003), pp. 693–699.
- [31] N. Yasuda and K. Fujita, *Effect of hydrostatic pressure on ferroelectric phase transition of lead scandium niobate*, Ferroelectrics 106 (1990), pp. 275–280.
- [32] M. Szafranski, A. Hilczer, and W. Nawrocik, *High-pressure peculiarities in Compositionally ordered $Pb(Sc_{1/2}Nb_{1/2})O_3$* , J. Phys. Condens. Matter 16 (2004), pp. 7025–7032.
- [33] A.A. Bokov, A. Hilczer, M. Szafranski, and Z.-G. Ye, *Impossibility of pressure-induced crossover from ferroelectric to nonergodic relaxor state in a $Pb(Mg_{1/3}Nb_{2/3})_{0.7}Ti_{0.3}O_3$ crystal: Dielectric spectroscopic study*, Phys. Rev. B 76 (2007), pp. 184116–1–14.
- [34] A.A. Bokov and Z.-G. Ye, *Phenomenological description of dielectric permittivity peak in relaxor ferroelectrics*, Solid State Commun. 116 (2000), pp. 105–108.
- [35] G.A. Samara, *Relaxor properties of compositionally disordered perovskites: Ba- and Bi-substituted $Pb(Zr_{1-x}Ti_x)O_3$* , Phys. Rev. B 71 (2005), pp. 224108–1–8.